Original article

Incorporation of iron into chloroplasts triggers the restoration of cadmium induced inhibition of photosynthesis

Ádám Solti[1*], Éva Sárvári[1], Brigitta Tóth[2], Ilona Mészáros[3], Ferenc Fodor[1]

[1]Department of Plant Physiology and Molecular Plant Biology, Institute of Biology, Faculty of Sciences, Eötvös Loránd University, Pázmány Péter sétány 1/C, Budapest, 1117, Hungary

[2] Department of Agricultural Botany, Crop Physiology and Biotechnology, Institute of Crop Sciences, Faculty of Agricultural and Food Sciences and Environmental Management, University of Debrecen, Böszörményi út 138, Debrecen, 4032, Hungary

[3]Department of Botany, Institute of Biology and Ecology, Faculty of Sciences and Technology, University of Debrecen, P.O. Box: 14 Debrecen, 4010 Hungary

*corresponding author: adam.solti@ttk.elte.hu

Abstract

Photosynthetic symptoms of acute Cd stress can be remedied by elevated Fe supply. To shed more light on the most important aspects of this recovery, the detailed Fe trafficking and accumulation processes as well as the changes in the status of the photosynthetic apparatus were investigated in recovering poplar plants. The Cd-free, Fe-enriched nutrient solution induced an immediate intensive Fe uptake. The increased Fe/Cd ratio in the roots initiated the translocation of Fe to the leaf with a short delay that led to the accumulation of Fe in the chloroplasts, finally. The chloroplast Fe uptake was directly proportional to the Fe translocation to leaves. The accumulation of PSI reaction centres and the recovery of PSII function studied by Blue-Native PAGE and chlorophyll *a* fluorescence induction measurements, respectively, began in parallel to the increase in the Fe content of chloroplasts. The initial reorganisation of PSII was accompanied with a peak in the antennae-based non-photochemical quenching. In conclusion, Fe accumulation of the chloroplasts is a process of prime importance in the recovery of photosynthesis from acute Cd stress.

Introduction

Many regions all over the world suffer from heavy metal pollution due to anthropogenic activities. Areas with high industrial or agricultural uses have to cope with increased soil cadmium (Cd) concentration (Nagajyoti et al., 2010). Cd has a known toxicity to the environment and to all plants (Sanità di Toppi and Gabbrielli, 1999), thus Cd contamination has increasing importance. Poplars (*Populus* spp.), which are able to tolerate Cd exposure, are economically important species from the point of view of phytoremediation.

In plants, Cd disturbs, among others, the homeostasis of several metals by competing essential metal uptake and translocation (Gallego et al., 2012). Cd stress leads to strong Fe-deficiency in the shoot (Siedlecka and Krupa, 1999; Fodor et al., 2005; Solti et al., 2008). Root-to-shoot Fe transport requires citrate for Fe(III)-citrate complex formation (Rellán-Álvárez et al., 2010). While Cd is supposed to translocate in non-chelated form, it reduced the expression of *AtFRD3* citrate transporter in *Arabidopsis* (Yamaguchi et al., 2010) leading to a diminished Fe translocation, and Fe deficiency in the shoot. In addition, the signalling pathways of the expression are disrupted and altered by the presence of Cd both in the roots (Besson-Bard et al., 2009; Wu et al., 2012) and in leaf tissues (Li et al., 2014). In contrast to the effects of Cd on root Fe uptake and translocation, its effects on the uptake of Fe across different membrane systems in the mesophyll cells is hardly known.

In the shoot, Cd toxicity and Cd induced Fe deficiency deeply influence the development and activity of the photosynthetic apparatus (Siedlecka and Krupa, 1999). Inhibition of the chlorophyll (Chl) biosynthesis is one of the causes of the retarded thylakoid development. Although Cd inhibits δ-ALA dehydratase directly, the main reason for the Cd-induced inhibition of Chl accumulation is the inhibition of Mg-protoporphyrin-IX-monomethyl-ester oxidative cyclase, which is an enzyme operating with Fe cofactor (Padmaja et al., 1990). Inhibition of Chl biosynthesis decreases the accumulation of all Chl-protein complexes

3

(Fagioni et al., 2009; Basa et al., 2014). Cd induced alterations in the photosynthetic structures are in many ways similar to those caused by Fe deficiency. As photosystem I (PSI) is the major Fe containing complex in the photosynthetic apparatus, Fe deficiency strongly retards the accumulation of PSI in the thylakoid membranes (Andaluz et al., 2006; Timperio et al., 2007; Basa et al., 2014). Strong inhibition of the photosynthetic electron transport is a general response to Cd stress. While PSI activity was less affected, Cd was shown to inhibit photosystem II (PSII) at molecular level (Sigfridsson et al., 2004). Functional disturbances of photochemical reaction centres lead to the generation and accumulation of reactive oxygen species (ROS) (Gallego et al., 2012). In the chloroplasts, one of the most important targets of ROS is the D1 protein of PSII. Damages in the PSII reaction centre leads to inactivation. Non-photochemical quenching (NPQ) pathways are essential to eliminate the surplus excitation energy thus prevent the generation of ROS. Among the variable quenching mechanisms, heat dissipation in antenna complexes and quenching by inhibited PSII centres can significantly contribute to NPQ (Hendrickson et al., 2005). Using internal non-photochemical quenching routes, the inactive reaction centres protect the neighbouring active PSIIs (Chow et al., 2005). Elevated level of Fe was shown to provide protection against many toxic effects of Cd. In the presence of Cd, increased Fe supply helped in retention of growth, pigments, and photosynthetic activity in bean and poplar seedlings (Siedlecka and Krupa, 1996; Sárvári et al., 2011). In *Brassica juncea*, the presence of Fe was found to protect thylakoid complexes against Cd compared to Fe deficient circumstances (Qureshi et al., 2010). In addition, it was also proved that a five-fold higher Fe supply was able to recover the acute Cd toxicity symptoms of photosynthesis (Solti et al., 2008), which also caused a Fe accumulation in the leaves independently of the presence of Cd in the nutrient solution. However, the exact reasons of this recovery: how and why this Fe accumulation starts and how does it contribute to the physiological restoration are not yet clear. Thus, our aim was to find out the

4

1 determining processes in this recovery. Therefore, the detailed dynamics of the Fe trafficking

2 and accumulation processes as well as the changes in the status of the photosynthetic

3 apparatus were investigated in recovering poplar plants.

4

5 **Materials and methods**

6

7 Plant material and treatments

8 Experiments were performed on micropropagated poplars (*Populus jacquemontiana* var.

9 *glauca* [Haines] Kimura cv. 'Kopeczkii'). Plants were grown in climatic chamber [14/10

10 hours light (100 µE m^{-2} s^{-1})/dark periods, 24/22 °C and 70/75% relative humidity] in

11 hydroponics of quarter-strength Hoagland solution [1.25 mM Ca(NO$_3$)$_2$, 1.25 mM KNO$_3$, 0.5

12 mM MgSO$_4$, 0.25 mM KH$_2$PO$_4$, 0.08 µM CuSO$_4$, 4.6 µM MnCl$_2$, 0.19 µM ZnSO$_4$, 0.12 µM

13 Na$_2$MoO$_4$, 11.56 µM H$_3$BO$_3$, and 10 µM Fe$^{(III)}$-citrate as iron source] for three weeks (four-

14 leaf stage). Low growth irradiance was necessary for the survival of Cd treated plants (Solti et

15 al., 2011). Then, non-treated control (Ctrl) plants were further grown under the same

16 conditions. A set of plants were treated with 10 µM Cd(NO$_3$)$_2$ for one week (Cad plants).

17 Nutrient solution was changed in every two days. To induce regeneration processes, Cd

18 treated plants were transferred to Cd-free nutrient solution containing a five-fold elevated Fe

19 supply (50 µM Fe$^{(III)}$-citrate; Cad/Ctrl50 plants). Recovery processes were followed on 6th

20 leaves, which developed entirely under Cd treatment and before the regeneration period.

21

22 Determination of chloroplast iron content

23 Intact chloroplasts of poplar leaves were isolated using a stepwise sucrose gradient, as

24 mentioned in Sárvári et al. (2011). Fe content of solubilised chloroplasts was measured in

25 reduced form as ferrous-bathophenantroline complex: [Fe(BPDS)$_3$]$^{4-}$ at 535 nm (ε=22.14 mM$^-$

1   [1] cm^{-1}) by UV-VIS spectrophotometer (Shimadzu, Japan). In order to normalize the Fe

2   content on a chloroplast number basis, images were taken on suspensions in a Bürker chamber

3   in Nikon Optiphot-2 microscope (Zeiss Apochromatic 40/0.95 160/0.17 objective) equipped

4   with Nikon *D*70 DSLR camera. Chloroplasts were counted using ImageJ software

5   (rsbweb.nih.gov/ij/) with Cell Counter plugin.

6

7   Determination of Fe concentration in the nutrient solution

8   Samples of 1 mL volume were taken from the 400 mL nutrient solution of the plants. After

9   reducing the whole available Fe content into Fe^{2+} form by adding 100 μM ascorbic acid, 300

10   μM BPDS was added to determine the Fe concentration according to the above mentioned

11   bathophenantroline method.

12

13   Determination of element concentrations

14   Leaves were dried for a week at 60 °C, powdered and digested using HNO_3 for 30 min at 60

15   °C, and then bleached by H_2O_2 for 90 min at 120 °C. After filtration through MN 640W

16   paper, element contents were measured by ICP-MS (Inductively Connected Plasma Mass

17   Spectrometer, Thermo-Fisher, USA).

18

19   Measurements of photosynthetic pigments

20   Chlorophyll content of leaves was determined in 80% (v/v) acetone extracts by a UV-VIS

21   spectrophotometer (Shimadzu, Japan) using the absorption coefficients of Porra et al. (1989).

22   For the quantification of xanthophyll cycle components, leaf discs were adapted to darkness

23   or to an actinic light of 100 μmol m^{-2} s^{-1} for 30 minutes, and stored in liquid nitrogen. Discs

24   were powdered in liquid nitrogen and extracted with 80% (v/v) acetone containing 0.1% (v/v)

25   NH_4OH at 4 °C. Carotenoid components were separated by HPLC method (Goodwin and

Britton, 1988) using a Nucleosil C18 column in HPLC-system equipped with an UV/VIS detector (JASCO Int. Co., Japan). The eluents were (i) acetonitrile:water mixture (9:1, 0.01% (v/v) triethylamine) and (ii) ethyl acetate. Zeaxanthin standard was used for the identification of peaks and calculation of pigment concentrations (Tóth et al., 2002). The de-epoxidation state of xanthophyll cycle pigments (DEEPS) was calculated as DEEPS=(Z+0.5A)/(V+A+Z), where V refers to the amount of violaxanthin, A to antheraxanthin and Z to zeaxanthin, respectively.

Separation and estimation of chlorophyll-protein complexes

Thylakoid membranes were isolated then solubilised, separated, identified and quantified as described by Sárvári et al. (2014). Shortly, after solubilisation with 2% (w/v) n-dodecyl-β-D-maltoside on ice for 30 min, 1st D electrophoresis was run using BlueNative PAGE (Kügler et al., 1997) in 5–12% (w/v) acrylamide gradient gels (Mini-Protean, BioRad) with 10–20 µl solubilized thylakoids (0.5 mg Chl ml^{-1}) applied per lane. Electrophoresis was carried out with constant voltage of 40 V (15 min), then 150 V and a maximum of 5 mA per gel at 6 °C for approximately 6 h. To analyse the polypeptide composition of the different complexes, thin slices of native gels were transferred to the top of denaturing gels, and run in second dimension by the method of Laemmli (1970) with a modification by adding 10% glycerol to the stacking (5%) and separating (10–18% linear gradient) gels. Complexes were identified by their characteristic polypeptide patterns as in Basa et al. (2014). Gels were scanned using an Epson Perfection V750 PRO gel scanner. The quantity of Chl-protein complexes were assessed according to the pixel density of the different bands in the 1st D BlueNative lanes using Phoretix 4.01 software (Phoretix International, Newcastle upon Tyne, UK). In the case of the complex PSI and PSII dimer band, the pixel number of PSII dimers was calculated proportionally to the pure PSII monomer band on the basis of the density ratio of CP47

apoproteins (PsbB) found in the complex and in the monomer PSII bands in the 2nd D gel pattern. Treatment-induced changes in the absolute amounts of complexes were estimated after the total pixel density of each lane was normalized to identical density (identical Chl content) and then to the total Chl content in leaves of differently treated plants (μg Chl leaf^{-1}).

Chlorophyll *a* fluorescence induction

Fluorescence induction measurements were carried out with intact leaves using a PAM 101-102-103 Chlorophyll Fluorometer (Walz, Effeltrich, Germany). Leaves were dark-adapted for 30 min. The F_0 level of fluorescence was determined by switching on the measuring light with modulation frequency of 1.6 kHz and photosynthetic photon flux density (PPFD) less than 1 μmol m^{-2} s^{-1} after 3 s illumination by far-red light in order to eliminate reduced electron carriers. The maximum fluorescence yields, F_m in the dark-adapted state and F_m' in light-adapted state, were measured by applying a 0.7 s pulse of white light (PPFD of 3500 μmol photon m^{-2} s^{-1}, light source: KL 1500 electronic, Schott, Mainz, Germany). The maximal and actual efficiency of PSII centres were determined as $F_v/F_m = (F_m - F_0)/F_m$ and $\Delta F/F_m' = (F_m' - F_t)/F_m'$, respectively. For quenching analysis, actinic white light (PPFD of 100 μmol photon m^{-2} s^{-1}, KL 1500 electronic) was provided. Simultaneously with the onset of actinic light the modulation frequency was switched to 100 kHz. The steady-state fluorescence of light-adapted state (F_t) was determined when no change was found in F_m' values between two white light flashes separated by 100 s. Considering that all stress factors inhibiting photosynthesis also leads to light stress, the quenching parameters of Hendrickson et al. (2005) were used for assessing the excitation energy allocation in all samples as follows:

$$\Phi_{PSII} = (1 - \frac{F_t}{F_m'}) * (\frac{F_v/F_m}{F_{vM}/F_{mM}}) ; \qquad \Phi_{NPQ} = (\frac{F_t}{F_m'} - \frac{F_t}{F_m}) * (\frac{F_v/F_m}{F_{vM}/F_{mM}}) ;$$

1 $$\Phi_{f,D} = (\frac{F_t}{F_m}) * (\frac{F_v / F_m}{F_{vM} / F_{mM}}) ; \qquad \Phi_{NF} = 1 - (\frac{F_v / F_m}{F_{vM} / F_{mM}}) ;$$

2

3 Φ_{PSII}: the photochemical efficiency of functional PSII centres; Φ_{NPQ}: ΔpH dependent,

4 xanthophyll-cycle coupled non-photochemical quenching; $\Phi_{f,D}$: fluorescence/thermal

5 dissipation of the absorbed energy; Φ_{NF}: the thermal dissipation by inactive PSII centres. The

6 intensity of actinic light (100 µmol photon m^{-2} s^{-1}) corresponded to the optimal growth light

7 intensity of Cad plants. F_{vM}/F_{mM} was applied as the mean of F_v/F_m values of Ctrl (quasi non-

8 inhibited) plants according Solti et al. (2014a).

9

10 Statistical analysis

11 The element and pigment contents of three individual plants per treatments were measured in

12 two subsequent experiments (n=6 biological repetitions). Thylakoid were isolated from five

13 plants per treatments in two subsequent experiments, and run by 2D BN/SDS PAGE 3 times

14 (2 biological and 3 technical repetitions per sample). To compare multiple treatments,

15 ANOVA tests with Tukey-Kramer multiple comparison *post hoc* tests were performed by

16 InStat v. 3.00 (GraphPad Software, Inc.). The term, 'significantly different', means that the

17 probability for similarity of samples is P<0.05.

18

19 **Results**

20

21 In order to study the detailed restoration process, growth, nutritional and photosynthetic

22 parameters of Cd treated plants were determined frequently after the transfer to Cd-free

23 nutrient solution containing a five-fold elevated Fe supply (Cad/Ctrl50 plants). In comparison,

24 the behaviour of Ctrl leaves was studied only at the beginning and the end of the short

1   investigating period to indicate the physiological characteristics of non-treated plants in

2   partially and totally developed leaves, and to address to which extent the values of parameters

3   in Cad/Ctrl50 leaves approximated the Ctrl level. Based on the previously reported data in

4   Solti et al. (2008), the continuous Cad (Cad/Cad) treatment was not repeated here since no

5   significant changes in the values of the parameters were detected in the period of the present

6   investigation.

7

8   Growth parameters

9   The 6th leaves of Ctrl plants reached their full physiological activity before the time of

10   investigations (Supplementary Table 1). Nevertheless, growth of leaves continued during the

11   recovery period. Cadmium treatment caused a significant decrease in the growth parameters

12   of 6th leaves compared to the Ctrl ones (Supplementary Table 1). Leaves reached about 75%

13   of their size up to the beginning of regeneration, and showed only a moderate increase further

14   during the recovery period. Both the growth of leaf area and dry weight terminated on the

15   third day of the recovery treatment. While the increase in fresh weight and leaf area was more

16   or less continuous (Fig. 1A, B), the dry weight accumulation was only significant during the

17   light period (Fig. 1C). Because of the slight increase in the growth parameters, we present the

18   physiological data on a leaf basis that represents the net changes occurred in whole leaves.

19

20   Uptake and translocation of Fe and Cd

21   After one-week Cd treatment, Fe concentration in the 6th leaves of treated poplar plants

22   decreased significantly compared to that of the corresponding Ctrl (Ctrl: 217.0±4.3 µg g^{-1}

23   DW; Cad: 102.0±2.8 µg g^{-1} DW, see also Supplementary Table 1). Transferring Cad plants to

24   a Cd-free, Fe-enriched nutrient solution, both the Fe uptake (measured as the remaining Fe

25   content of the nutrient solutions; Fig. 2) and translocation (measured as the Fe content of

leaves; Fig. 3A) increased significantly. The Fe uptake was clearly associated to the light periods both in Ctrl and Cad/Ctrl50 plants as no change in the Fe concentration of the nutrient solutions was found before and after the dark periods (Fig. 2). The relative intensity of the uptake of Fe in both Ctrl and Cad/Ctrl50 plants was maximal in the first light period, and decreased in parallel to the decline of the Fe content of the nutrient solution. Similarly to Ctrl plants, Cad/Ctrl50 plants also removed more or less the total Fe content from their 400 mL nutrient solution during the 72 h regeneration period, which means a 3.83 ± 0.13 µmol (Ctrl) and 19.26 ± 0.26 µmol (Cad/Ctrl50) net Fe uptake from the total 4 and 20 µmol available Fe content, respectively.

Fe content of the 6th leaves of Cad/Ctrl50 plants started to increase following a 3 h lag-period. It only increased during the light periods, while the Fe content of leaves was the same before and after the dark periods (Fig. 3A). The intensity of Fe accummulation in leaves was the highest during the second light period (400.5 ± 6.2 µg Fe leaf^{-1} accumulated in an hour, in average). In contrast to Fe content, Cd content of 6th leaves was more or less stable in the light, and an increase was detected between the end of the previous and the start of the next light periods (Fig. 3B). .

One-week Cd treatment significantly decreased the Fe content of the chloroplasts compared to Ctrls (Supplementary Table 1). The Fe content of chloroplasts of Cad/Ctrl50 plants also increased only in the light periods (Fig. 3C). Although chloroplast Fe content started to rise in the first light period, this increase was significantly higher during the second and third light periods. As a result of three-day recovery, the Fe content of chloroplast in 6th leaves of Cad/Ctrl50 plants reached the Ctrl level measured at the beginning of the recovery period (Supplementary Table 1). The Fe content of chloroplasts in Ctrl plants also increased together with plant growth.

Fe translocation and chloroplast Fe accumulation were analysed as the function of the root Fe

uptake or root Fe/Cd ratio and as the function of leaf Fe content or the amount of translocated

Fe, respectively. These analyses indicated that the Fe translocation into the leaves and Fe

uptake of chloroplast were directly proportional to the Fe taken up by roots and by leaves,

respectively (Fig. S1). Translocation to the 6th leaf started when the Fe/Cd ratio in roots was

≥ 2 on a dry weight basis (Fig. 4A). Chloroplast Fe uptake was first detected when the Fe

concentration in the 6th leaf exceeded about 2 nmol Fe mg^{-1} DW (Fig. 4B).

Restoration of photosynthetic pigments

The amount of Chl pigments significantly decreased under acute Cd stress (Supplementary

Table 1). The Fe-enriched recovery medium caused a restoration in the pigment pool. The

total Chl content (Chl *a*+*b*) remained unchanged and increased during the first and second

light period, respectively (Fig. 5A). However, a slight increase in the standard deviation of the

Chl content at the end of the first light period also indicates the initiation of Chl accumulation,

which, perhaps, was interrupted by the dark period. A slow but gradual Chl accumulation was

found during the subsequent light periods. As a result of this increase, the total Chl content in

Cad/Ctrl50 leaves approximated the level of Ctrl before the recovery period in three days

(Supplementary Table 1). Higher amount of Chls was found in Ctrl leaves in a growth-

dependent manner.

The Chl *a*/*b* ratio of treated leaves changed markedly by the elevated Fe supply (Fig. 5B). Cd

treatment caused a significant decrease in Chl *a/b* ratio which started to increase in parallel to

the rise in chloroplast Fe content. The Chl *a/b* ratio exceeded the level of Ctrl in the second

light period, then lowered back to the level of Ctrl. Later on, no further oscillations were

measured. No similar variability was observed in the Chl *a/b* ratio of Ctrl leaves (data not

shown).

The amount of carotenoids decreased significantly in Cad leaves compared to Ctrls (Supplementary Table 1). Carotenoid content also showed characteristic changes in 6th leaves of Cad/Ctrl50 plants. The amount of β-carotene stagnated in the initial phase of recovery but turned into accumulation in the third part of the first light period (Fig. 6A). During the second light period, some accumulation was also observed, then no further significant changes were measured in the β-carotene content. In contrast to the β-carotene, both of the lutein and the ΣVAZ contents remained unchanged during the first light period, and started to increase only later in the second light period (Fig. 6B,C). Afterwards, no singnificant changes were observed. Carotenoid content of Ctrl leaves increased significantly during the recovery treatment without any change in the caroteinoid composition (Supplementary Table 1).

In Cad/Ctrl50 leaves, the change in the de-epoxidation of xanthophyll cycle pigments under light adapted conditions (DEEPS) showed similar trend to that of the Chl a/b ratio (Fig. 6D). It started to increase in the first light period, reached its maximum in the second ligh period and began to decrease markedly from the end of the second light period gradually reaching the level of the Ctrl.

Chl-protein composition of thylakoid membranes

The main Chl-containing bands separated by Blue-Native PAGE, after resolution of their individual proteins by SDS PAGE, were identified as PSI (supercomplexes and monomers, both contain PSI subcomplexes), PSII supercomplexes (contain PsbB, PsbC, and Lhcb antennae), PSII dimers and monomers (contain PsbB, PsbC), PSII complexes that lack CP43 (contains PsbB, but not PsbC), Lhc supercomplex (LHCII that also bind connecting antennae), Lhc complexes and monomers (contain Lhcb trimers and/or Lhcb proteins) (Fig. 7A,B).

The amount and ratio of each complexes were strongly altered under acute Cd stress compared to Ctrl: the amount of all complexes were reduced, and a retardation in the relative abundance of LHCII trimers and PSI complexes was observed (Supplementary Table 2, Fig. 7C). Starting up the recovery, the complexes showed characterisctic changes in the 6th leaves of Cad/Ctrl50 plants (Fig. 7C, Fig. 8). Accumulation of reaction centres (both PSI and PSII) could be detected from the beginning of the second light period, in parallel to the increase in the chloroplast Fe concentration, while the amount of LHCII timers and Lhc monomers increased mainly from the second part of the second light period accompanied by the decrease in the Chl a/b ratio (Fig. 8, black arrows). However, remarkable changes were already observed in the macrocomplex organisation of PSII in the very early phase of recovery, practically in parallel to the start of the increase in the Fe content of leaves and chloroplasts. Reorganisation of PSII complexes and their antenna was evidenced by the elevated amounts of PSII supercomplexes, PSII dimers and Lhc supercomplexes (Fig. 8, grey arrows). By the time of 53. hour of the recovery, the abundance of PSII complexes, Lhc supercomplexes and LHCII trimers more or less approached the level of the initial value (0 h) of the Ctrl leaves, whereas the amount of PSI complexes still remained well below the Ctrl value (Supplementary Table 2). In the Ctrl leaves, together with Chl accumulation, all thylakoid complexes increased in abundance during the investigated time period. Some reorganization of the thylakoids, i.e. the elevated ratio of supercomplexes was also observed.

Excitation energy allocation

Control plants reached their full physiological activity before the start of recovery as it was proved by the observed stability in the excitation energy allocation parameters during the recovery period (Supplementary Table 1). In contrast, acute Cd stress caused strong decrease in the photochemical quenching (Φ_{PSII}), and elevated the constant thermal dissipation and

14

fluorescence ($\Phi_{f,D}$) and non-photochemical quenching by inactive PSII reaction centres (Φ_{NF}). During recovery treatment, the Φ_{PSII} started to rise slowly but tendentiously (Fig. 9A). By the third light period, there was no significant difference between Cad/Ctrl50 and Ctrl leaves. The tendency of changes in both $\Phi_{f,D}$ and Φ_{NF} were roughly the opposite compared to Φ_{PSII} parameter but the relaxation of $\Phi_{f,D}$ was faster than that of Φ_{NF} (Fig. 9C,D). Though acute Cd stress did not cause any significant changes in the antennae-based non-photochemical quenching, the start of the recovery processes was clearly associated with a peak-like elevation of Φ_{NPQ} values approximately 6-10 hours after the start of regeneration at the end of the first light period (Fig. 9B). In the second light period, the Φ_{NPQ} values of regenerating plants did not differ from those of the Ctrls'. Altogether, the most important changes were associated with the 6-11 h time window after exposure to elevated Fe level.

Discussion

Acute cadmium stress resulted in inhibited Fe accumulation in leaves thus causing disturbed development of the photosynthetic apparatus (Siedlecka and Krupa, 1999; Solti et al., 2008). By increasing the Fe supply of Cd stressed poplar plants, an appropriate sequence of restoration processes was observed in Fe uptake and translocation, chloroplast Fe uptake, and in the recovery of photosynthetic parameters.

Uptake and translocation of Fe

After replacing the nutrient solution to Cd-free, Fe-enriched medium (Cad/Ctrl50 plants), the Fe content of roots, leaves and chloroplasts became elevated in a short time period. Increase in the Fe translocation and in the chloroplast Fe uptake were directly proportional to the Fe uptake by roots and Fe translocation to leaves, respectively, i.e. dependent on the actual Fe flux into the roots and to the leaves.

15

Concerning the Fe uptake, the Fe content of the fresh nutrient solution decreased without any delay (Fig. 2) indicating that the Cd stress does not inhibit the Fe uptake of the roots. The total Fe content of the medium was taken up by both the Ctrl and Cad/Ctrl50 plants (4 and 20 µmol Fe in the 400 mL nutrient solution, respectively) during three light periods, which underlines the importance of the periodic nutrient solution refreshments in experimental protocols. Moreover, the decrease in the Fe content of Ctrl50 solution was much higher compared to Ctrl, which must be connected to the fast increase in the Fe concentration of root tissues of Cad/Ctrl50 plants. The high Fe uptake intensity of Cad/Ctrl50 roots found in this work also supports that the activity/number of Fe uptake-related enzymes/transporters (NtIRT1 and NtFRO1 orthologs) were higher in the roots of Cad than in Ctrl plants, as it was also shown at expression level by Yoshihara et al. (2006). In agreement, Cad treatment induced an accumulation of not only Cd but also Fe in the roots (Fodor et al., 2005). The dependence of root Fe uptake on light periods may be related to the fact that root carbon metabolism and root exudation strongly depends on the phloem carbon import, and thus on photosynthesis (Dilkes et al., 2004). The Fe uptake is probably source-limited (organic acids and reducing power) during the dark periods. Shoot-born signals also contribute to the diurnal regulation of Fe uptake related proteins in strategy-I plants (Vert et al., 2003). Moreover, the Fe nutritional status also has a feedback regulation on the circadian clock (Hong et al., 2013)

With a short delay to the Fe uptake, Fe translocation also started in regenerating plants (Fig. 3). The decreased leaf Fe, which is a well-known indirect effect of Cd treatment (Siedlecka and Krupa, 1999), started to increase after a three-hour lag period probably connected to a delay in the root-to-shoot Fe translocation. The short delay indicates that the regulation of Fe translocation may be in strong interaction with the increase in the Fe/Cd ratio of root symplast from 0.3, characteristic to Cad plants (Fodor et al., 2005), to around 2.0 (Fig 4A). The quasi-continuous Cd translocation to leaves (from the Cd reservoir of roots) and the

strong Fe uptake of roots caused a shift in Fe/Cd ratio which probably affected the Fe-related signal transduction pathways. Since the xylem loading of Fe is strongly dependent on the presence of citrate (Rellán-Álvarez et al., 2010), and Cd stress decreases the amount of the FRD3 citrate transporter significantly (Yamaguchi et al., 2010), the increasing translocation of Fe could be a result of enhanced transcription of *AtFrd3 Populus* ortholog (Durrett et al., 2007). Similarly to Fe uptake, Fe translocation also seems to have a diurnal activity as the citrate is converted from sugar and sugar alcohol molecules transported to the roots in the phloem. At the same time, the effect of the root pressure may be the dominant impulsive force in Cd translocation.

The majority of shoot Fe content is localised in the chloroplasts, particularly in thylakoids (Morrissey and Guerinot, 2009). As a result of acute Cd stress and also under Fe deficiency, the Fe content of chloroplasts decreased in accordance with previous data (Sárvári et al., 2011; Basa et al., 2014). The effect of Cd on Fe transport mechanisms inside the mesophyll cells is poorly known. Under acute Cd stress, the reduced Fe uptake of chloroplasts is connected to (i) the inhibited photosynthetic activity and the direct coupling of the photosynthetic electron transport and the reduction-based Fe uptake mechanism of chloroplast (Solti et al., 2014b) and (ii) the possible preferred mitochondrial Fe uptake under Fe limited conditions (Vigani, 2012, Vigani et al., 2013). Nevertheless, during regeneration, the short (approximately 5-6 hours) delay between the start of leaf and chloroplast Fe accumulation and the direct proportionality between Fe translocation and chloroplast Fe uptake together indicate that chloroplast Fe uptake is preferred if more Fe (at least around 2 nmol mg^{-1} DW) is available in the leaf (Fig. 4B), and consequently, in the cytoplasm of the mesophyll cells. Based on our data, the further translocation of Cd to the leaf could have negligible impact on the chloroplast Fe acquisition process. In agreement, the presence of a large amount of Cd in chloroplasts has not been verified yet (Ramos et al., 2002; Pietrini et al., 2003).

Restoration of photosynthetic structures and activity

It has long been known that the reasons for many symptoms of acute Cd stress are indirect, the most serious one, in the context of photosynthetic structures and activity, being the Cd induced Fe deficiency (Siedlecka and Krupa, 1999; Solti et al., 2008). Together with the inhibition of Chl synthesis, the accumulation of PSI complexes was inhibited primarily, but the development of PSII and particularly its antenna system was also retarded under Cd treatment (Fagioni et al., 2009; Basa et al., 2014) as well as under Fe deficiency (Timperio et al., 2007; Basa et al., 2014). Since the amount of PSII complexes were the least sensitive to Cd stress, the markedly lowered PSII activity (decreased Φ_{PSII}) is connected to the presence of damaged PSII reaction centres verified by the high proportion of quenching related to non-functional PSII reaction centres (high Φ_{NF}). As a result of Cd stress, the amount and aggregation of Lhc complexes also decreased (Fig. 8, Basa et al., 2014). Similarly, reduced amount of Lhcb1 and Lhcb2 proteins was also observed in rye under similar conditions, which significantly decreased the Chl-Chl and Chl-carotenoid energy transfer rate (Janik et al., 2010). The declined efficiency of excitation energy transfer may be the main reason for the elevated $\Phi_{f,D}$ values in Cad plants.

During regeneration, together with the increase in the chloroplast Fe content (Fig. 3), both the accumulation of Chl-protein complexes and their structural remodelling and functional restoration were observed (Fig. 8). The Chl *a/b* ratio and the amount of *β*-carotene increased first indicating the accumulation of reaction centres. According to the analysis of pigment-protein complexes, the main reason was the sharp elevation in the amount of the Fe containing PSI reaction centres. As the biosynthesis of Chls and Fe-S cofactor binding proteins such as the PSI reaction centre requires a significant amount of Fe (Jensen et al., 2003; Amunts et al., 2010), the start of their accumulation is an indirect sign of the elevation

of bioactive Fe content in chloroplasts. According to a recent discovery in *Chlamydomonas reinhardtii*, the nuclear-encoded TAA1 protein may contribute to the sensing of the chloroplast Fe nutritional status and contribute to the expression of *PsaA* gene (Lefebvre-Legendre et al., 2015). The delay we measured under the recovery treatment between the uptake of Fe into the chloroplasts and the appearance the PsaA was similar to that found in *Chlamydomonas*. Nevertheless, the presence of TAA1 homologs in higher plants has not been proved yet.

Lowering of the Chl *a/b* ratio and increase in the amounts of lutein and other xanthophylls, i.e. the accumulation of Chl *a+b* containing Lhc antennae, mostly LHCII trimers, was delayed to the second light period. Together with the accumulation of thylakoid complexes, the actual quantum efficiency (Φ_{PSII}) also recovered gradually in parallel to the decrease in excitation energy dissipation by inactive PSII reaction centres (Φ_{NF}). In addition to the decreasing Φ_{NF} values, other processes also indicate the remodelling of the different non-photochemical quenching routes. A sharp, peak-like increase in the antennae based non-photochemical quenching (Φ_{NPQ}) observed in the third part of the first light period of recovery coincided with the fast reorganisation of complexes (elevated ratio of PSII dimers, PSII- and Lhc supercomplexes) without a net increase in their amounts (Fig. 9C vs. Fig. 8). Thus, the reorganisation of PSII may have contributed to this peak Φ_{NPQ} values.

Conclusion

The root-to-shoot Fe translocation and the Fe uptake of chloroplasts is retarded under a threshold value of root and leaf Fe content (or Fe/Cd ratio), respectively. During the recovery of Cd stressed plants performing high Fe-uptake capacity, the elevated Fe supply starts a rapid Fe accumulation in the roots. The increase in the root Fe/Cd ratio induces root-to-leaf Fe translocation, and the increased Fe content of leaves enhances Fe uptake into the chloroplasts.

Accumulation of Fe in chloroplasts precedes the recovery of photosynthesis independently of the presence and further translocation of Cd to the leaf. Among the Fe homeostasis linked structural and physiological parameters, the biogenesis of PSI complexes and the remodelling and reactivation of PSII complexes are the most important in the initialization of the restoration of photosynthesis.

Acknowledgements

References

Amunts, A., Toporik, H., Borovikova, A., Nelson, N. 2010. Structure determination and improved model of plant photosystem I. J. Biol. Chem. 285, 3478–3486.

Andaluz, S., López-Millán, A-F., de las Rivas, J., Aro, E-M., Abadía, J., Abadía, A., 2006. Proteomic profiles of thylakoid membranes and changes in response to iron deficiency. Photosynth. Res. 89, 141–155.

Basa, B., Lattanzio, G., Solti, Á., Tóth, B., Abadía, J., Fodor, F., Sárvári, É., 2014. Changes induced by cadmium stress and iron deficiency in the composition and organization of thylakoid complexes in sugar beet (*Beta vulgaris* L.). Environ. Exp. Bot. 101, 1–11.

Besson-Bard, A., Gravot, A., Richaud, P., Auroy, P., Duc, C., Gaymard, F, Taconnat, L., Renou, J-P., Pugin, A., Wendehenne, D., 2009. Nitric oxide contributes to cadmium

toxicity in *Arabidopsis* by promoting cadmium accumulation in roots and by up-regulating genes related to iron uptake. Plant Physiol. 149, 1302–1315.

Chow, W.S., Lee, H.Y., He, J., Hendrickson, L., Hong, Y.M., Matsubara, S., 2005. Photoinactivation of photosystem II in leaves. Photosynth. Res. 84, 35–41.

Dilkes, N.B., Jones, D.L., Farrar, J., 2004. Temporal dynamics of carbon partitioning and rhizodeposition in wheat. Plant Physiol. 134, 706–715.

Durrett, T.P., Gassmann, W., Rogers, E.E., 2007. The FRD3-mediated efflux of citrate into the root vasculature is necessary for efficient iron translocation. Plant Physiol. 144, 197–205.

Fagioni, M., D'Amici, G.M., Timperio, A.M., Zolla, L., 2009. Proteomic analysis of multiprotein complexes in the thylakoid membrane upon cadmium treatment. J. Proteome Res. 8, 310–326.

Fodor, F, Gáspár, L, Morales, F, Gogorcena, Y, Lucena, JJ, Cseh, E, Kröpfl, K, Abadía, J, Sárvári, É., 2005. The effect of two different iron sources on iron and cadmium allocation in cadmium exposed poplar plants (*Populus alba* L.). Tree Physiol. 25, 1173–1180.

Gallego, S.M., Pena, L.B., Barcia, R.A., Azpilicueta, C.E., Iannone, M.F., Rosales, E.P., Zawoznik, M.S., Groppa, M.D., Benavides, M.P., 2012. Unravelling cadmium toxicity and tolerance in plants: Insight into regulatory mechanisms. Environ. Exp. Bot. 83, 33–46.

Goodwin, T.W., Britton, G. 1988. Distribution and analysis of carotenoids, in: Goodwin, T.W. (Ed.), Plant pigments. Academic Press, London, UK, pp. 62–132.

Hendrickson, L., Förster, B., Pogson, B.J., Chow, W.S., 2005. A simple chlorophyll fluorescence parameter that correlates with the rate coefficient of photoinactivation of Photosystem II. Photosynth. Res. 84, 43–49.

1   Hong, S., Kim, S.A., Guerinot, M.L., McClung C.R. 2013. Reciprocal interaction of the

2   circadian clock with the iron homeostasis network in *Arabidopsis*. Plant Physiol. 161,

3   893-903.

4   Janik, E., Maksymiec, W., Mazur, R., Garstka, M,. Gruszecki, W.I., 2010. Structural and

5   functional modifications of the major light-harvesting complex II in cadmium or

6   copper-treated *Secale cereale*. Plant Cell Physiol. 51, 1330–1340.

7   Jensen, P.E., Haldrup, A., Rosgaard, L., Scheller, H.V. 2003. Molecular dissection of

8   photosystem I in higher plants: topology, structure and function. Physiol. Plant. 119,

9   313–321.

10   Kügler, M., Jänsch, L., Kruft, V., Schmitz, U.K., Braun, H.P., 1997. Analysis of the

11   chloroplast protein complexes by blue-native polyacrylamide gel electrophoresis (BN-

12   PAGE). Photosynth. Res. 53, 35–44.

13   Laemmli, U.K., 1970. Cleavage of structural proteins during assembly of the head of

14   bacteriophage T4. Nature 227, 680–685.

15   Lefebvre-Legendre, L., Choquet, Y., Kuras, R., Loubéry, S., Douchi D., Goldschmidt-

16   Clermont, M. 2015. A nucleus-encoded chloroplast protein regulated by iron

17   availability governs expression of the photosystem I subunit PsaA in *Chlamydomonas*

18   *reinhardtii*. Plant Physiol. 167, 1527-1540.

19   Li, J., Liu, B., Cheng, F., Wang, X., Aarts, M.G.M,. Wu, J., 2014. Expression profiling

20   reveals functionally redundant multiple-copy genes related to zinc, iron and cadmium

21   responses in *Brassica rapa*. New Phytol. 203, 182–194.

22   Morrissey J, Guerinot ML., 2009. Iron uptake and transport in plants: The good, the bad, and

23   the ionome. Chem. Rev. 109, 4553–4567.

24   Nagajyoti, P.C., Lee, K.D., Sreekanth, T.V.M., 2010. Heavy metals, occurrence and toxicity

25   for plants: a review. Environ. Chem. Lett. 8, 199–216.

Padmaja, K., Prasad, D.D.K., Prasad, A.R.K., 1990. Inhibition of chlorophyll synthesis in *Phaseolus vulgaris* L. seedlings by cadmium acetate. Photosynthetica 24, 399–405.

Pietrini, F., Iannelli, M.A., Pasqualini, S., Massacci, A. 2003. Interaction of cadmium with glutathione and photosynthesis in developing leaves and chloroplasts of *Phragmites australis* (Cav.) Trin. ex Steudel. Plant Physiol. 133, 829-837.

Porra, R.J., Thompson, W.A., Kriedman, P.E., 1989. Determination of accurate excitation coefficient and simultaneous equations for assaying chlorophylls *a* and *b* extracted with four different solvents: verification of the concentration of chlorophyll standards by atomic absorption spectroscopy. Biochim. Biophys. Acta 975, 384–394.

Qureshi, M.I., D'Amici, G.M., Fagioni, M., Rinalducci, S., Zolla, L., 2010. Iron stabilizes thylakoid protein–pigment complexes in Indian mustard during Cd-phytoremediation as revealed by BN-SDS-PAGE and ESI-MS/MS. J. Plant Physiol. 167, 761–770.

Rellán-Álvarez, R., Andaluz, S., Rodríguez-Celma, J., Wohlgemuth, G., Zocchi, G., Álvarez-Fernández, A., Fiehn, O., López-Millán, A-F., Abadía J., 2010. Changes in the proteomic and metabolic profiles of *Beta vulgaris* root tips in response to iron deficiency and resupply. BMC Plant Biol. 10, 120.

Ramos, I., Esteban, E., Lucena, J.J., Gárate, A. 2002. Cadmium uptake and subcellular distribution in plants of *Lactuca* sp. Cd-/Mn interaction. Plant Sci. 162, 761-776.

Sanità di Toppi, L., Gabbrielli, R., 1999. Response to cadmium in higher plants. Environ. Exp. Bot. 41, 105–130.

Sárvári, É., Solti, Á., Basa, B., Mészáros, I., Lévai, L., Fodor, F., 2011. Impact of moderate Fe excess under Cd stress on the photosynthetic performance of poplar (*Populus jaquemontiana* var. *glauca* cv. Kopeczkii). Plant Physiol. Biochem. 49, 499–505.

Sárvári, É., Mihailova, G., Solti, Á., Keresztes, Á., Velitchkova, M., Georgieva K., 2014. Comparison of thylakoid structure and organization in sun and shade *Haberlea*

rhodopensis populations under desiccation and rehydration. J. Plant Physiol. 171, 1591–1600.

Siedlecka, A., Krupa, Z., 1996. Interaction between cadmium and iron and its effectson photosynthetic capacity of primary leaves of *Phaseolus vulgaris*. Plant Physiol. Biochem. 34, 833–841.

Siedlecka, A., Krupa, Z., 1999. Cd/Fe interaction in higher plants – its consequences for the photosynthethic apparatus. Photosynthetica 36, 321–331.

Sigfridsson, K.G.V., Bernát, G., Mamedov, F., Styring, S., 2004. Molecular interference of Cd^{2+} with photosystem II. Biochim. Biophys. Acta 1659, 19–31.

Solti, Á., Gáspár, L., Mészáros, I., Szigeti ,Z., Lévai, L., Sárvári, É., 2008. Impact of iron supply on the kinetics of recovery of photosynthesis in Cd-stressed poplar (*Populus glauca*). Ann. Bot. 102, 771–782.

Solti, Á., Gáspár, L., Vági, P., Záray, G., Fodor, F., Sárvári, É., 2011. Cd, Fe, and light sensitivity: Interrelationships in Cd-treated *Populus.* OMICS – J. Integr. Biol. 15, 811–818.

Solti, Á., Lenk, S., Mihailova, G., Mayer, P., Barócsi, A., Georgieva, K., 2014a. Effects of habitat light conditions on the excitation quenching pathways in desiccating *Haberlea rhodopensis* leaves: an Intelligent FluoroSensor study. J. Photochem. Photobiol. 130C, 217–225.

Solti Á., Müller B., Czech V., Sárvári É., Fodor F. 2014b. Functional characterization of the chloroplast ferric chelate oxidoreductase enzyme. New Phytol 202, 920–928.

Timperio, A.M., D'Amici, G.M., Barta, C., Loreto, F., Zolla, L., 2007. Proteomics, pigment composition, and organization of thylakoid membranes in iron-deficient spinach leaves. J. Exp. Bot. 58, 3695–3710.

1   Tóth, V.R., Mészáros, I., Veres, Sz., Nagy, J., 2002. Effects of the available nitrogen on the

2   photosynthetic activity and xanthophyll cycle pool of maize in field. J. Plant Physiol.

3   159, 627–634.

4   Vert, G.A., Briat, J-F., Curie C. 2003. Dual regulation of the Arabidopsis high-affinity root

5   iron uptake system by local and long-distance signals. Plant Physiol. 2003 132, 796–

6   804.

7   Vigani, G., 2012. Discovering the role of mitochondria in the iron deficiency-induced

8   metabolic responses of plants. J. Plant Physiol. 169, 1–11.

9   Vigani, G., Zocchi, G., Bashir, K., Philippar, K., Briat, J-F. 2013. Signals from chloroplasts

10   and mitochondria for iron homeostasis regulation. Trends Plant Sci. 18, 305–311.

11   Wu, H., Chen, C., Du, J., Liu H., Cui, Y., Zhang, Y., He, Y., Wang, Y., Chu, C., Feng, Z., Li,

12   J., Ling, H-Q., 2012. Co-overexpression FIT with AtbHLH38 or AtbHLH39 in

13   *Arabidopsis*-enhanced cadmium tolerance via increased cadmium sequestration in

14   roots and improved iron homeostasis of shoots. Plant Physiol. 158, 790–800.

15   Yamaguchi, H., Fukuoka, H., Arao, T., Ohyama, A., Nunome, T., Miyatake, K., Negoro, S.,

16   2010. Gene expression analysis in cadmium-stressed roots of a low cadmium-

17   accumulating solanaceous plant, *Solanum torvum*. J. Exp. Bot. 61, 423–437.

18   Yoshihara, T., Hodoshima, H., Miyano, Y., Shoji, K., Shimada, H., Goto, F., 2006. Cadmium

19   inducible Fe deficiency responses observed from macro and molecular views in

20   tobacco plants. Plant Cell Rep. 25, 365–373.

21
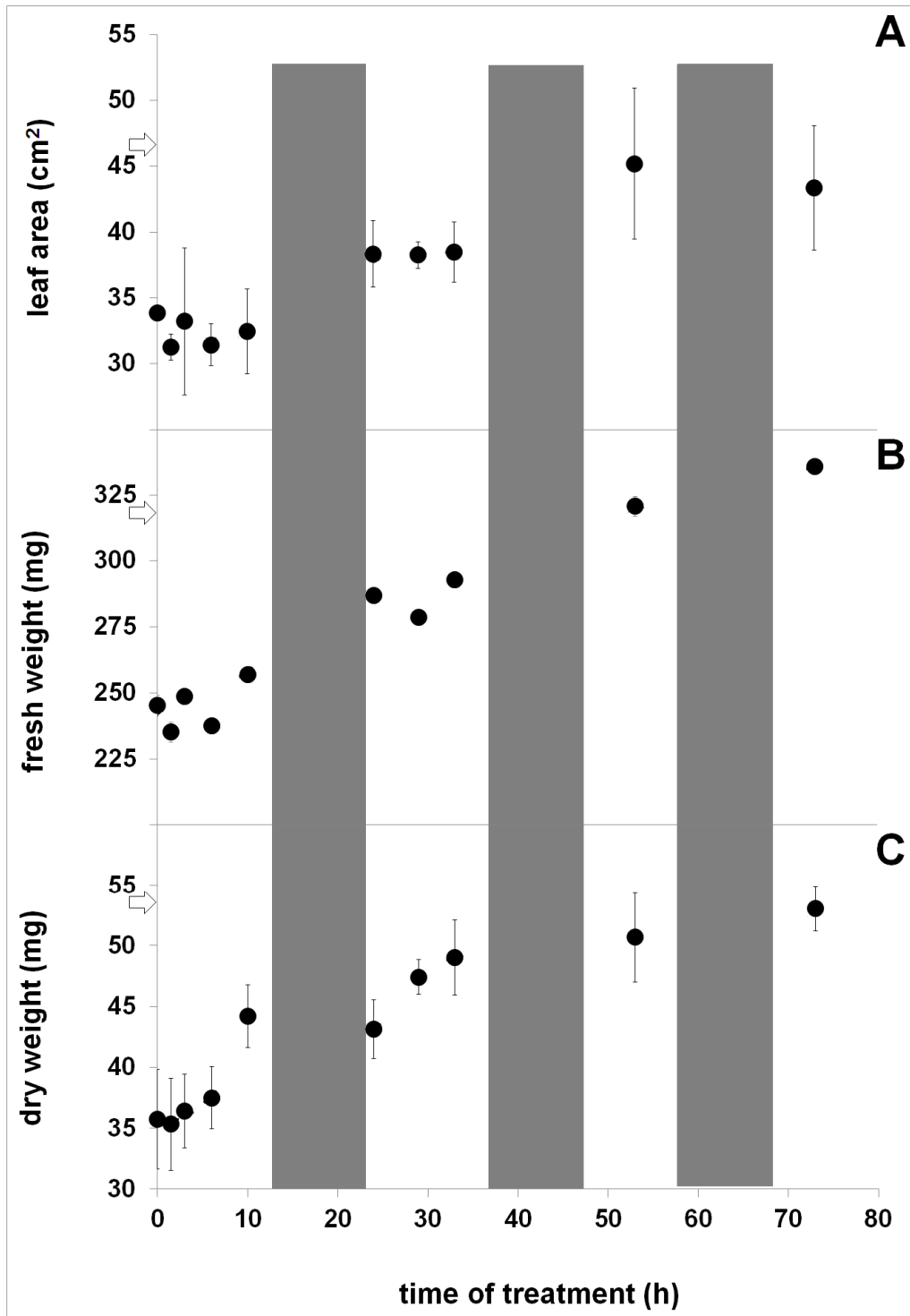
Figure 1. Area growth (A) and increase in fresh (B) and dry weight (C) of Cad/Ctrl50 leaves during the recovery period. Ctrl values at the beginning of the recovery treatment are indicated by arrows. Grey fields indicate the dark periods and the error bars show the SD, n=6.
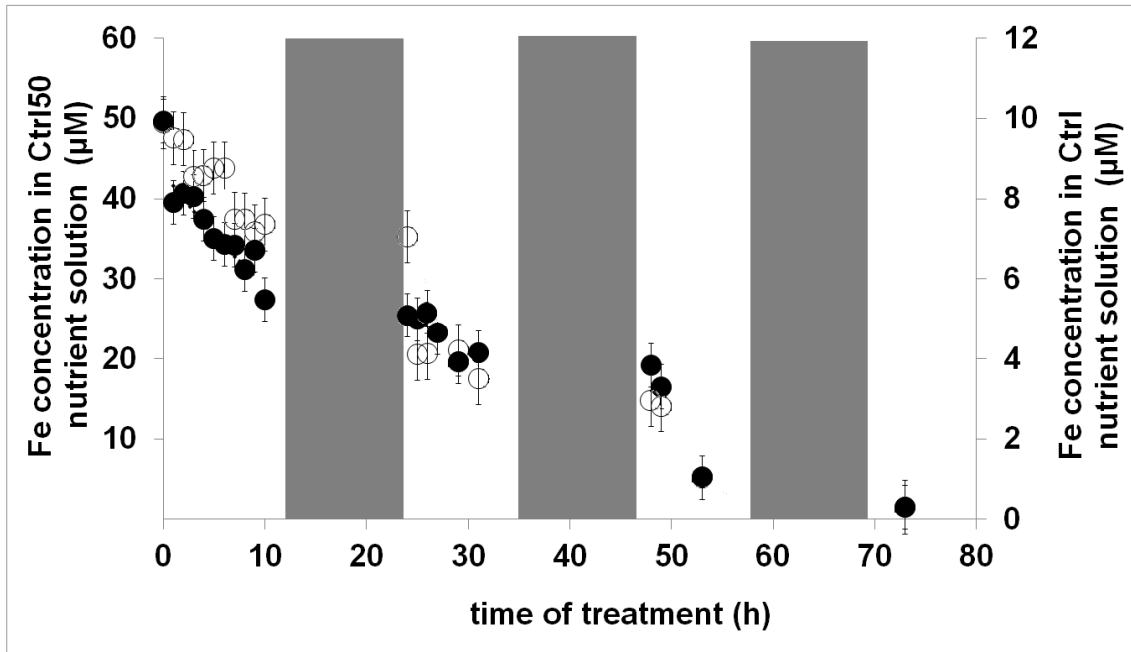
Figure 2. Changes in the Fe concentration in the nutrient solutions of Ctrl (open circles) and Cad/Ctrl50 (closed circles; after transferring the plants to a Cd-free nutrient solution) plants. Grey fields indicate the dark periods and the error bars show the SD, n=6.
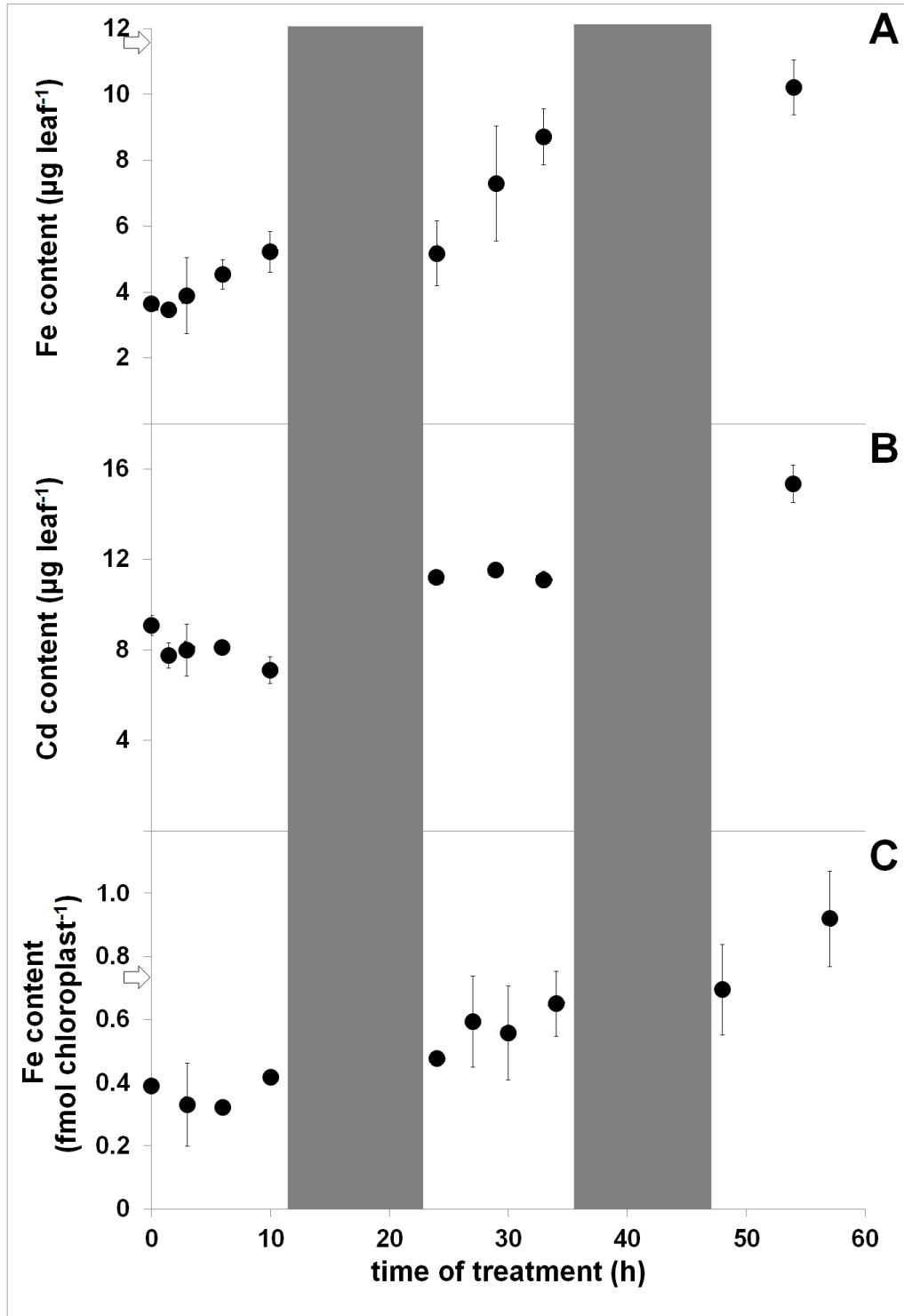
Figure 3. Changes in the Fe (A) and Cd (B) content of 6th leaves, and the Fe content of chloroplasts (C) in Cad/Ctrl50 plants during the recovery period. Ctrl values at the beginning of the recovery treatment are indicated by arrows. Cd content in Ctrl leaves was below the limit of detection. Grey fields indicate the dark periods and the error bars show the SD, n=6.
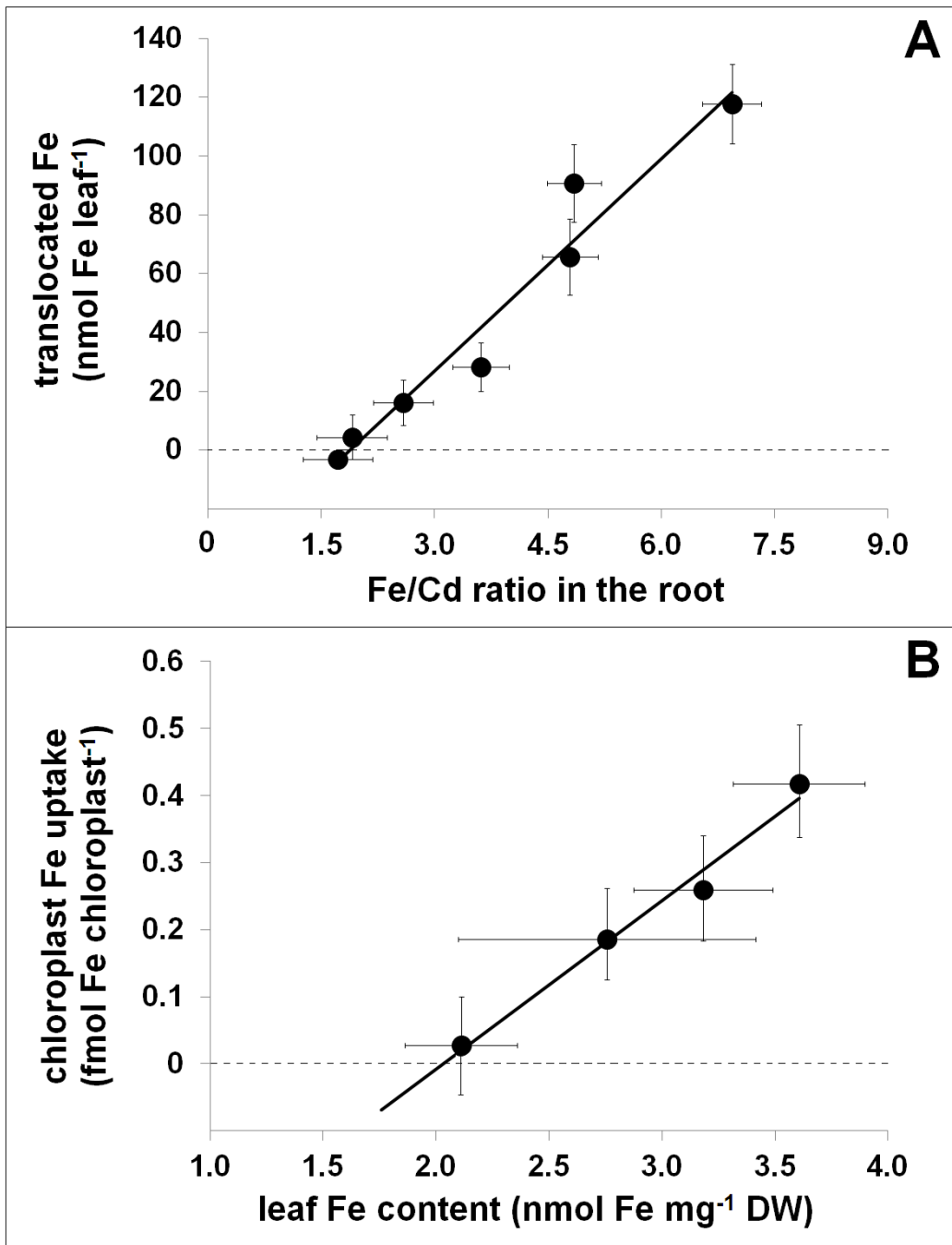
Figure 4. Dependence of root-to-leaves Fe translocation and chloroplast Fe uptake on the Fe/Cd ratio in roots (A) and the leaf Fe content (B), respectively. For the correlation analysis between the parameters, linear regressions were performed, where R^2 values were (A): 0.9523 and (B): 0.9825. Error bars represent SD values.
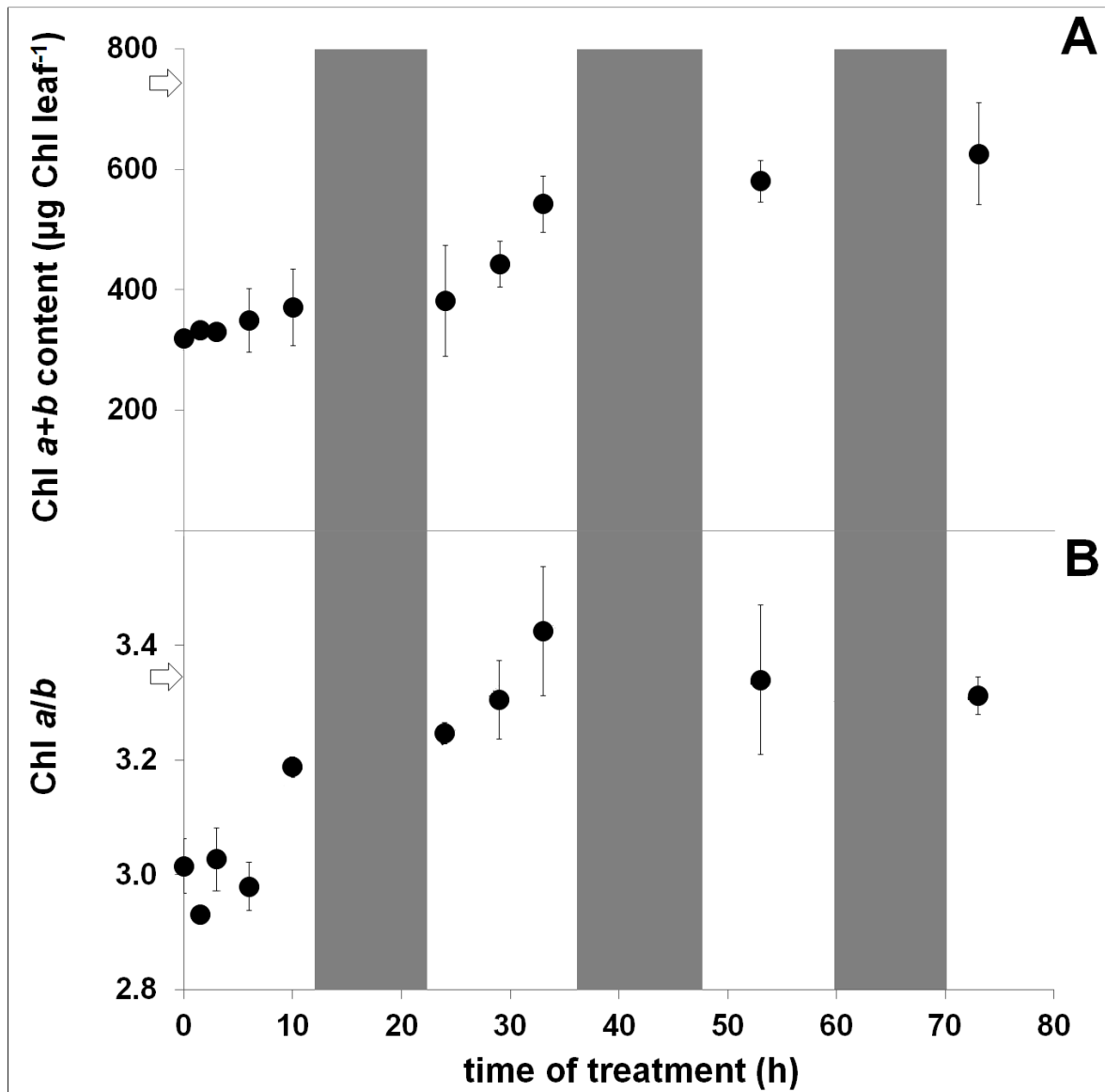
Figure 5. Changes in the total Chl content (A) and Chl *a/b* ratio (B) in 6th leaves of Cad/Ctrl50 plants during the recovery period. Ctrl values at the beginning of the recovery treatment are indicated by arrows. Grey fields indicate the dark periods and the error bars show the SD, n=6.
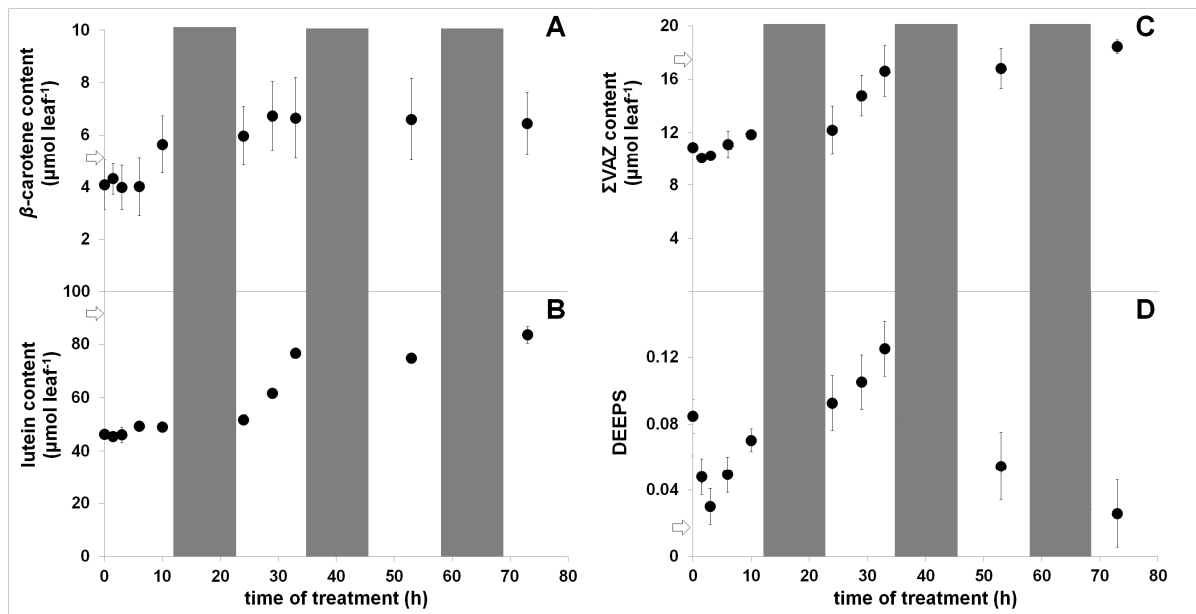
1

2   **Figure 6.** Changes in the amount of *β*-carotene (A), lutein (B), and ΣVAZ (C) pigments, and

3   the de-epoxidation of light-adapted xanthophyll cycle pigment pool (DEEPS; D) in 6th leaves

4   of Cad/Ctrl50 plants during the recovery period. Ctrl values at the beginning of the recovery

5   treatment are indicated by arrows. Grey fields indicate the dark periods and the error bars

6   show the SD, n=6.
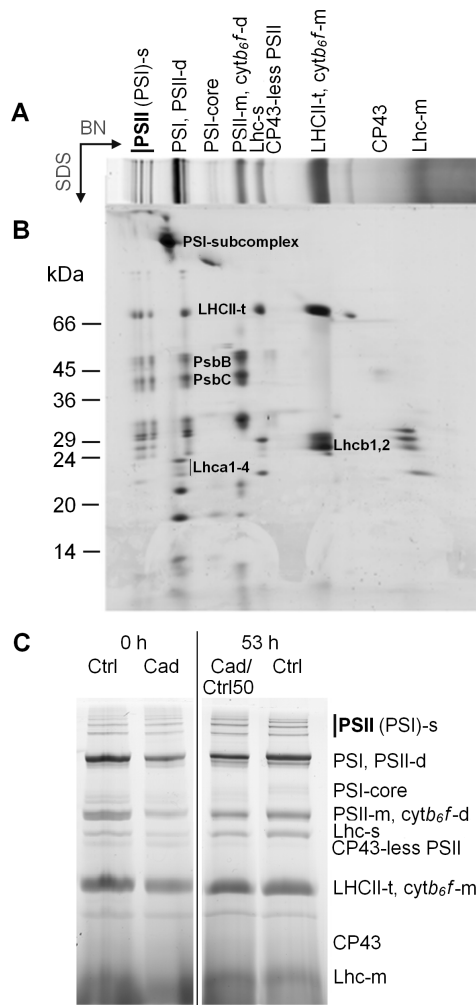
Figure 7. Separation and analysis of thylakoid membrane complexes by 2D BlueNative/SDS PAGE. (A) 1^{st}D BlueNative PAGE profile of a representative control thylakoid membrane. The identified protein complexes are indicated. (B) 2^{nd}D SDS PAGE: polypeptide patterns of the same representative control thylakoid membrane complexes. Characteristic proteins used to identify complexes are indicated. (C) Representative differences in the composition of thylakoid membranes isolated from 6th leaves of Ctrl, Cad and Cad/Ctrl50 plants at the beginning (0 h) and the end (53 h) of the recovery treatment, respectively. Abbreviations: BN – BlueNative; LHC/Lhc – light-harvesting complex, PS – photosystem; cyt b_6/f – cytochrome b_6/f complex, CP – chlorophyll-protein, s – supercomplex, t – trimer, d – dimer, m – monomer.
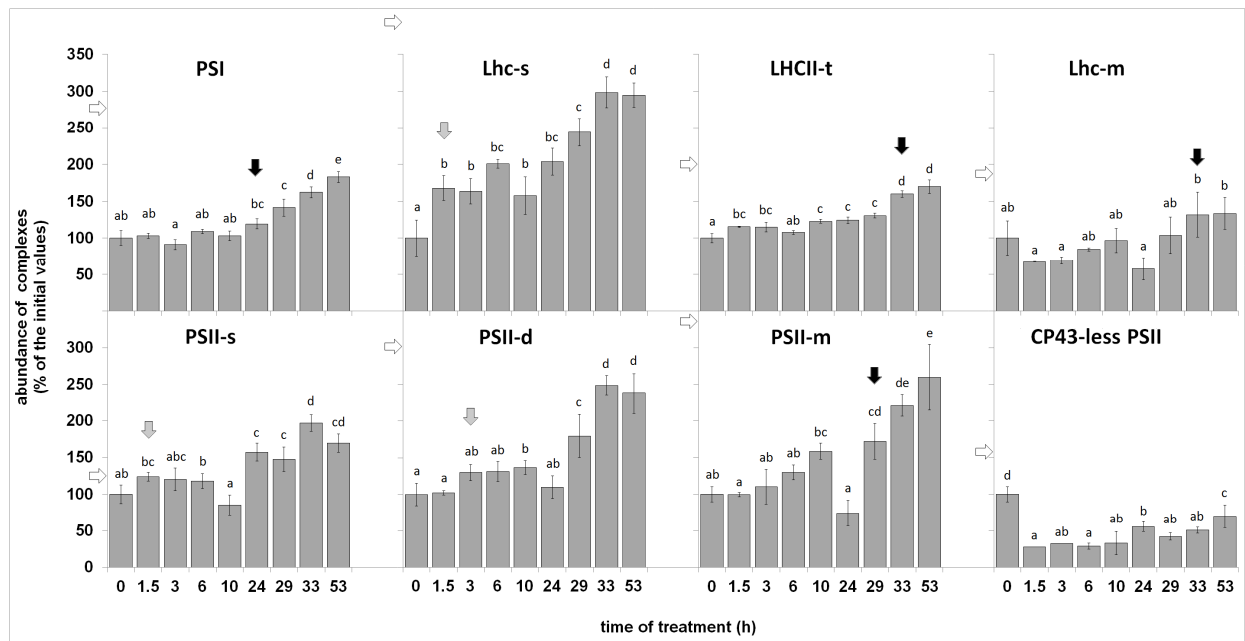
Figure 8. Changes in the amount of Chl-protein complexes in 6th leaves of Cad/Ctrl50 plants during the recovery period given in the percentage of the initial values (0 h treatment time). For starting and end values see: Supplementary Table 2. Abbreviations: Lhc-s – Lhc supercomplex; LHCII-t –Lhcb trimer (LHCII complex); Lhc-m –Lhcb monomer; PSII-s – PSII supercomplex; PSII-d – PSII dimer; PSII-m – PSII monomer; CP43-less PSII – PSII complexes lacking CP43. Filled arrows indicate the first sign of accumulation of the complexes: grey arrow – first light period; black arrow – second light period. Ctrl values at the beginning of the recovery treatment are indicated by open arrows. Erros bars indcate SD values, n=6.
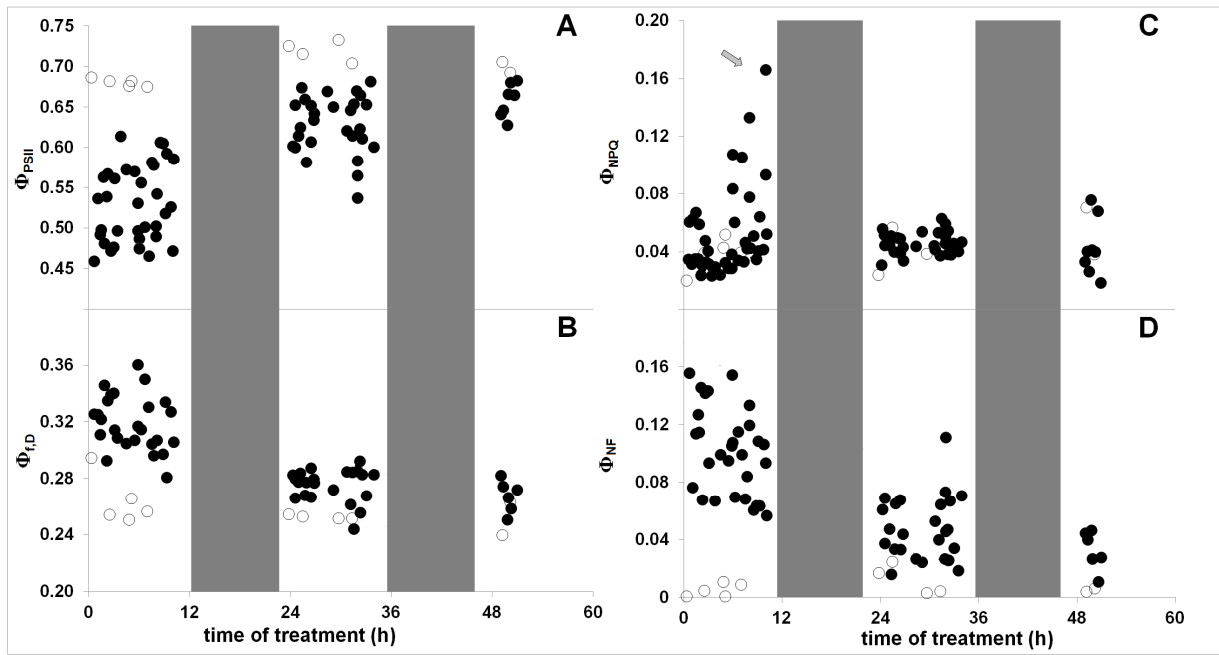
Figure 9. Changes of the Φ_{PSII} (A), $\Phi_{f,D}$ (B), Φ_{NPQ} (C) and Φ_{NF} (D) parameters in 6th leaves of Ctrl (open circles) and Cad/Ctrl50 plants (closed circles) during the recovery period. Data points represent single measurements from a sample population of five plants per treatment. Grey fields indicate the dark periods and the erros bars shows the SD, n=6. Arrow shows the peak values of Φ_{NPQ} around 6-10 hours of recovery.

Supplement

2

Supplementary Table 1. Physiological parameters of the 6th leaves at the beginning and in the 53. hour of the investigated recovery period. Treatments: Ctrl – control or Cad – one week treatment without or with 10 µM CdNO$_3$ in Hoagland solution of ¼ strength, 53 h Ctrl or Cad/Ctrl50 – further treatment under Ctrl conditions or with five-fold elevated Fe supply. Similarities between samples (n=6) were analysed with one-way ANOVA with *post-hoc* Tukey-Kramer test (P<0.05).

	0 h		53 h	
	Ctrl	Cad	Ctrl	Cad/Ctrl50
leaf area (cm^2)	46.7±3.9^a	33.9±0.4^b	85.1±4.4^c	45.2±5.7^a
fresh weight (mg)	320.9±19.2^a	245.2±56.2^b	597.1±22.6^c	320.7±46.4^a
dry weight (mg)	53.8±3.2^a	35.7±4.0^b	100.0±3.8^c	50.7±3.7^a
leaf Fe content (µg leaf^{-1})	11.7±0.2^a	3.6±0.1^b	22.0±0.4^c	8.7±0.8^d
chloroplast Fe content (fmol chloroplast^{-1})	0.74±0.24^a	0.40±0.13^b	1.22±0.19^c	0.81±0.15^a
leaf Cd content (µg leaf^{-1})	n.d.	9.0±0.4^a	n.d.	11.1±0.4^b
Chl *a+b* content (µg leaf^{-1})	736.8±172.8^{ac}	319.6±7.2^b	1568.5±91.0^c	580.3±34.6^a
Chl *a/b* ratio	3.40±0.01^a	3.01±0.05^b	3.32±0.04^a	3.34±0.13^a
β-carotene content (µmol leaf^{-1})	5.03±0.95^{ab}	4.07±0.94^a	10.32±1.72^c	6.59±1.57^b
lutein content (µmol leaf^{-1})	92.9±5.5^a	46.3±1.3^b	197.6±0.8^c	74.6±1.2^c
ΣVAZ (µmol leaf^{-1})	17.2±1.1^a	10.9±1.7^b	34.1±1.2^c	16.8±1.5^a
DEEPS	0.018±0.002^a	0.068±0.006^b	0.021±0.002^c	0.037±0.008^a
Φ_{PSII}	0.698±0.020^a	0.521±0.040^b	0.699±0.009^a	0.658±0.021^a
Φ_{NPQ}	0.041±0.009^a	0.040±0.016^a	0.054±0.023^a	0.045±0.020^a
$\Phi_{f,D}$	0.258±0.014^a	0.315±0.021^b	0.251±0.017^a	0.266±0.011^a
Φ_{NF}	0.004±0.004^a	0.124±0.038^b	0.001±0.007^a	0.031±0.013^a

9

10

1 **Supplementary Table 2.** Abundance of Chl-protein complexes (values given in µg Chl leaf

2 ^{1}) in the differently treated 6th leaves. Treatments: Ctrl – control or Cad – one week treatment

3 without or with 10 µM CdNO$_3$ in Hoagland solution of ¼ strength, 53 h Ctrl or Cad/Ctrl50 –

4 further treatment under Ctrl conditions or with five-fold elevated Fe supply. Abbreviations:

5 LHC/Lhc – light-harvesting complexes, PS – photosystem; CP – chlorophyll-protein, s –

6 supercomplex, t – trimer, d – dimer, m - monomer. Similarities between samples (n=6) were

7 analysed with one-way ANOVA with *post-hoc* Tukey-Kramer test (P<0.05).

	0 h		53 h	
	Ctrl	Cad	Ctrl	Cad/Ctrl50
PSI	189.6±2.9^a	68.7±7.9^b	386.6±11.3^c	125.6±5.1^d
PSII-s	30.5±4.5^{ab}	24.5±3.1^a	152.3±7.5^c	41.5±3.0^b
PSII-d	49.7±3.0^b	16.3±5.9^a	126.3±15.2^c	38.7±4.5^b
PSII-m	89.7±1.8^a	25.3±2.6^b	151.0±7.5^c	65.8±11.4^d
CP43-less PSII	16.3±4.5^a	10.2±1.1^{ab}	14.1±5.0^a	7.1±1.6^b
Lhc-s	30.9±9.6^b	7.9±2.3^a	109.3±2.4^c	27.1±1.5^b
LHCII-t	214.3±7.5^b	107.3±6.8^a	434.6±43.7^c	182.1±9.9^b
Lhc-m	83.0±3.1^a	44.8±10.4^a	128.0±41.2^b	59.8±9.6^a

8
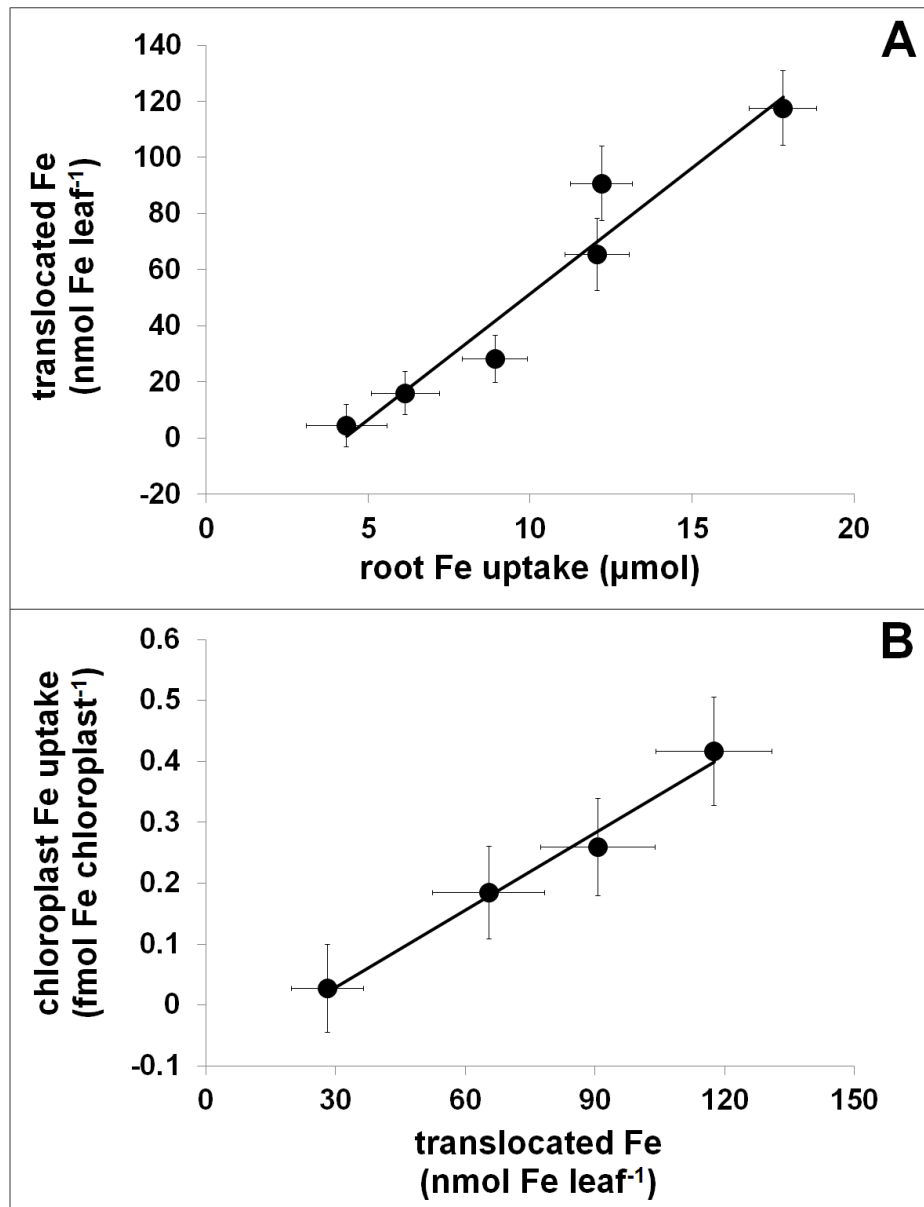
1

2   **Supplementary Figure 1.** Dependence of Fe translocation and chloroplast Fe uptake on the

3   Fe uptake of roots (A) and the root-to-leaf Fe translocation (B), respectively. The values

4   measured during the lag periods with no significant uptake and translocation were omitted

5   from this evaluation. As for correlation analysis between the parameters, linear regressions

6   were performed, where R^2 values were (A): 0.9393 and (B): 0.9863. Thus, it can be concluded

7   that Fe translocation into the leaves as well as Fe uptake into the chloroplasts is directly

8   proportional to the Fe taken up by roots and by leaves, respectively.

9